In utero delivery of miRNA induces epigenetic alterations and corrects pulmonary pathology in congenital diaphragmatic hernia

Sarah J. Ullrich,[1] Nicholas K. Yung,[1] Tory J. Bauer-Pisani,[1] Nathan L. Maassel,[1] Mary Elizabeth Guerra,[1] Mollie Freedman-Weiss,[1] Samantha L. Ahle,[1] Adele S. Ricciardi,[1,2] Maor Sauler,[3] W. Mark Saltzman,[2,4,5,6] Alexandra S. Piotrowski-Daspit,[2] and David H. Stitelman[1]

[1]Department of Surgery, Yale University, New Haven, CT 06510, USA; [2]Department of Biomedical Engineering, Yale University, New Haven, CT 06511, USA; [3]Department of Medicine, Yale University, New Haven, CT 06510, USA; [4]Department of Chemical & Environmental Engineering, Yale University, New Haven, CT 06511, USA; [5]Department of Cellular & Molecular Physiology, Yale University, New Haven, CT 06511, USA; [6]Department of Dermatology, Yale University, New Haven, CT 06510, USA

Structural fetal diseases, such as congenital diaphragmatic hernia (CDH) can be diagnosed prenatally. Neonates with CDH are healthy *in utero* as gas exchange is managed by the placenta, but impaired lung function results in critical illness from the time a baby takes its first breath. MicroRNA (miR) 200b and its downstream targets in the TGF-β pathway are critically involved in lung branching morphogenesis. Here, we characterize the expression of miR200b and the TGF-β pathway at different gestational times using a rat model of CDH. Fetal rats with CDH are deficient in miR200b at gestational day 18. We demonstrate that novel polymeric nanoparticles loaded with miR200b, delivered *in utero* via vitelline vein injection to fetal rats with CDH results in changes in the TGF-β pathway as measured by qRT-PCR; these epigenetic changes improve lung size and lung morphology, and lead to favorable pulmonary vascular remodeling on histology. This is the first demonstration of *in utero* epigenetic therapy to improve lung growth and development in a pre-clinical model. With refinement, this technique could be applied to fetal cases of CDH or other forms of impaired lung development in a minimally invasive fashion.

INTRODUCTION

Congenital diaphragmatic hernia (CDH) results from incomplete fusion of the diaphragm *in utero* causing the abdominal organs to herniate into the chest cavity.[1,2] It is a relatively common condition with an incidence of 1 in 2,000 to 3,000 live births.[3,4] Even with modern neonatal critical care, the overall mortality is approximately 30%, and approaches 80% for those with severe disease.[5,6] Infants with CDH have poorly developed lungs with two predominant pathologic features: pulmonary hypoplasia (PH) characterized by reduced distal airway branching with fewer alveoli, which are thick walled and have persistent pulmonary hypertension due to hypermuscularized arterioles that are less vasoactive.[7–10]

There is a compelling rationale to develop fetal intervention for CDH given the potential to reverse PH *in utero*, before the delivered fetus takes its first breath. Trials examining fetoscopic endoluminal tracheal occlusion (FETO), where a balloon is deployed in the trachea under fetoscopic guidance and subsequently removed weeks later, have demonstrated a survival benefit for those with severe disease.[11,12] Among fetuses treated with FETO, those who had subsequent lung growth and survived after balloon deployment and retrieval had higher microRNA (miR) 200b expression in their tracheal fluid aspirates than those who did not respond to tracheal occlusion.[13] The microRNA 200 family inhibits several genes in the transforming growth factor β (TGF-β) pathway, which has been previously demonstrated to modulate lung branching during development, and *in vitro* studies suggest that treatment with miR200b can induce TGF-β/SMAD signaling and increase branching morphogenesis.[13–18]

miRNAs are rapidly degraded by serum enzymes and intracellular RNases, making them highly unstable *in vivo*.[19] For miRNAs to be used therapeutically, it is essential for them to be delivered in a vehicle that confers high stability and avoids potential toxicities.[20,21] A variety of approaches have been explored to address these limitations, such as chemically modifying the miRNA mimics to enhance stability or using viral vectors, lipid emulsions, liposomes, lipid nanoparticles (NPs), or polymeric NPs.[19,22–29] But stabilized miRNA mimics have decreased mRNA silencing ability, viral vectors have a poor safety profile, and cationic lipids are toxic to cells and pro-inflammatory.[19,30] Polymeric NPs can be used for the sustained delivery of drugs, are non-toxic with a low side effect profile, and can be optimized to target fetal lung.[31–33] We have recently demonstrated that polymeric NPs can safely be used to deliver editing reagents in the form of peptide nucleic acids and donor DNAs *in utero* to correct a disease-causing mutation in the β-globin gene in a mouse model of human β-thalassemia.[34] Optimization for delivery to fetal lung
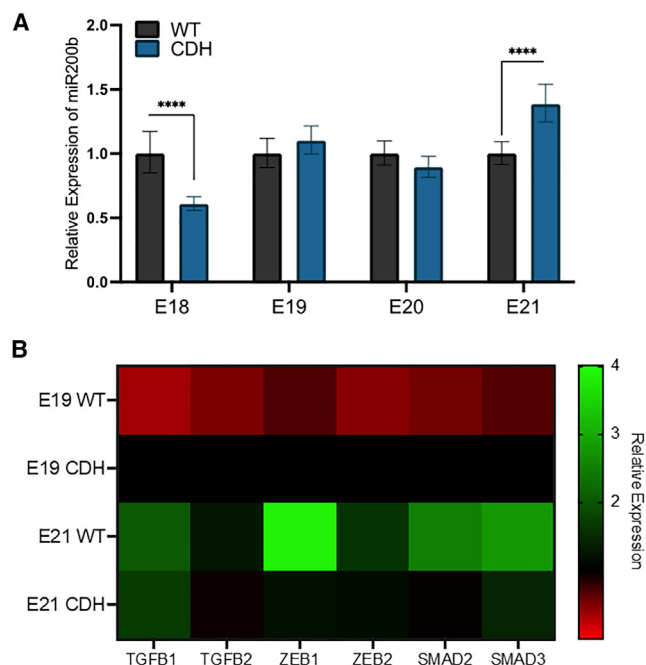
Figure 1. miR200b and TGF-β pathway expression during the canalicular and saccular phases of lung development in the Nitrofen rat model of CDH

(A) Bar graph showing the relative abundance of miR200b in wild-type (WT) and CDH lungs during late gestation. All values normalized to WT at each day. Student's t test, ****p < 0.0001. Data are shown as mean ± SD of n = 10–12. (B) Heatmap of the relative expression of the TGF-β pathway during the canalicular (E19) and saccular (E21) phases of pulmonary development in WT and CDH lungs. Red, downregulated; green, upregulated. n = 4.

demonstrated that intravenous delivery led to improved lung delivery over intra-amniotic delivery, and that cationic poly(amine-co-ester) (PACE) NPs were delivered most efficiently to fetal lung.[33]

Here, we sought to deliver miR200b in utero using PACE NPs to treat a rat model of CDH. We found that in utero delivery of miR200b induces alterations in the TGF-β pathway, leads to pulmonary vascular remodeling, and improves PH.

RESULTS

miR200b expression and TGF-β signaling is altered during late gestation in the nitrofen model of CDH

Branching morphogenesis of fetal rat lung is completed during the canalicular stage of lung development (E18 through E20), whereas the terminal airspaces develop and divide during the saccular stage (E21–P4).[35] It has been demonstrated previously that miR200b regulates distal airway branching, and that at E18 miR200b expression is reduced in nitrofen-exposed lungs, and at E21 miR200b expression is increased in nitrofen-exposed lungs.[17,18] To determine an ideal therapeutic window for in utero miR delivery, we further elucidated the temporal expression of miR200b in the wild-type (WT) and nitrofen-induced CDH lungs. The relative expression of miR200b in WT and CDH lungs were quantified using qRT-PCR. In WT fetal rat

lung, miR200b levels are stable during the canalicular phase and undergo a 1.7-fold increase at the transition to the saccular phase (Figure 1A). In CDH lungs, there is a 40% decrease in the relative expression of miR200b at E18 during the early canalicular stage (Figure 1A). During the mid and late canalicular phase, there is no difference in the relative expression of miR200b between WT and CDH lungs. At E21, the relative expression of miR200b is 1.4-fold greater in CDH lungs compared with WT lungs.

The TGF-β signaling pathway is a regulator of branching morphogenesis in pulmonary development and is modulated by miR200b.[36,37] The role of the TGF-β pathway in CDH is less clearly defined.[38] We found that, in WT lungs, the expression of TGF-β and its downstream targets increases as the lungs transition from the canalicular to the saccular phase (Figure 1B) (statistical comparison provided in Table S1). In CDH lungs, the expression of TGF-β and its downstream targets is increased during the canalicular phase compared with WT lungs. In CDH lungs, the TGF-β pathway does not undergo the same increase in expression during late development, with the relative expression of most downstream targets remaining stable between E19 and E21.

The minority of nitrofen-treated rat fetuses have PH without CDH; these PH rats do not have the same deficiency in miR200b at those with CDH at E18, although the levels of miR200b are different in PH and CDH later in pregnancy (Figure S1A). In addition, WT and PH lungs have differences in expression of the TGF pathway at E19 and E21 (Figures S1B and S1C).

In utero delivery of miR200b induces epigenetic changes

Because we found that miR200b levels were reduced in CDH lungs at E18, we elected to target this time point for treatment. Our previous data demonstrated that the majority of nucleic acid release from PACE60 NPs occurs within the first 24 h.[39] To align delivery of miR200b with the appropriate therapeutic window, we injected NPs at E17. To validate if in utero injection of miRNA PACE60 NPs led to an increase in miR200b levels, WT fetuses were injected with control or miR200b-loaded NPs. Lungs were evaluated 4 h after injection. Those injected with miR200b had a 12-fold increase in miR200b levels (Figure 2A). Naked, unencapsulated miR200b delivered at the same dose at E17 is undetectable in fetal rat lung at 4 h (Figure S2).

Previous in vitro studies demonstrated that treatment with a miR200b mimic abrogates nitrofen-induced upregulation of the TGF-β pathway.[18] We performed a toxicity study and found that NP doses of 30 mg/kg were safe with high levels of survival to full term (Figure S3). We treated nitrofen-exposed pups with control or miR200b NPs at E17 and assessed the relative expression of the TGF-β pathway using qRT-PCR at E19 and E21. We found that pups with CDH who were treated with miR200b PACE60 NPs had a decrease in the relative expression of TGF-β1 and SMAD2 at E19 compared with pups treated with control NPs (Figure 2B). At E21, pups treated with miR200b had a decrease in TGF-β1 expression and SMAD3 expression compared with those treated with control NPs (Figure 2C). There were no instances where pups treated with control NPs had a
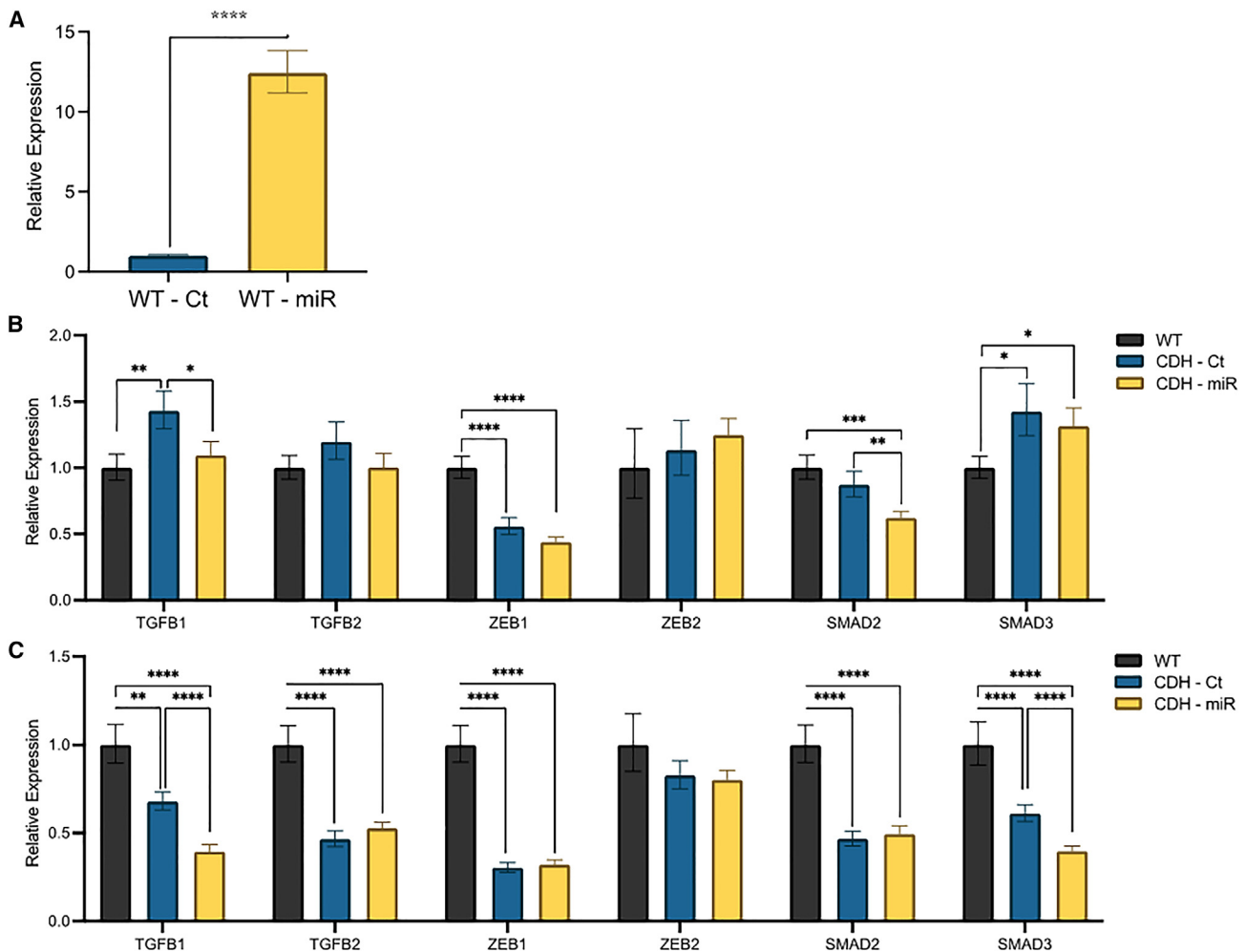
Figure 2. _In utero_ delivery of miR200b by PACE60 NPs alters miR200b expression levels and induces epigenetic changes related to the TGF-β pathway
(A) Bar graph showing the relative abundance of miR200b in WT fetal lungs at E17 4 h post injection with control and miR200b PACE60 NPs. Values normalized to lungs injected with control miRNA PACE NPs. Student's t test, ****$p < 0.0001$. Data are shown as mean ± SD of $n = 3$. (B) Bar graph showing the relative abundance of the downstream targets of the TGF-β pathway in WT fetal lungs and those injected with control miRNA and miR200b PACE60 NPs at E19. Values normalized to WT lungs. Two-way ANOVA, *$p < 0.05$, **$p < 0.01$, ***$p < 0.001$, ****$p < 0.0001$. Data are shown as mean ± SD of $n = 4–6$. (C) Bar graph showing the relative abundance of the downstream targets of the TGF-β pathway in WT fetal lungs and those injected with control miRNA and miR200b PACE60 NPs at E21. Values normalized to WT lungs. Two-way ANOVA, **$p < 0.01$, ****$p < 0.0001$. Data are shown as mean ± SD of $n = 4–6$.

change in gene expression and miR200b PACE60 NPs did not. By full term, the levels of miR200b in the lung of CDH pups that received miR200b-loaded NPs at E17 were comparable with full-term WT lungs (Figure S4).

In fetuses with PH without CDH, we do not see significant changes in TGF-β signaling in the PH treated with miR200b NPs and those that are untreated (Figure S5).

Lung morphology improves after _in utero_ treatment with miR200b
To assess if _in utero_ treatment with miR200b lead to morphometric changes in fetal lung, lungs of CDH pups were harvested at E21 after

treatment with either control or miR200b PACE60 NPs at E17. Treatment with miR200b improved PH in pups with CDH (Figures 3A–3C). The lung to body weight ratios of pups treated with miR200b NPs increased by 27% (2.2% vs. 2.8%), and approached the ratios of WT pups (3.4%, Figure 3D). Pulmonary airspace improved 140% in pups treated with miR200b, approaching that of WT pups, as measured by mean linear intercept (WT 37 μM, control 11 μM, miR200b 26 μM, Figure 3E). In addition, pups treated with miR200b had a 63% decrease in mean alveolar thickness, decreased beyond that of WT pups (WT 9 μM, control 16 μM, miR200b 6 μM, Figure 3F).

In utero treatment with miR200b also led to pulmonary vascular remodeling (Figures 4A–4C). The pulmonary arteries of pups injected
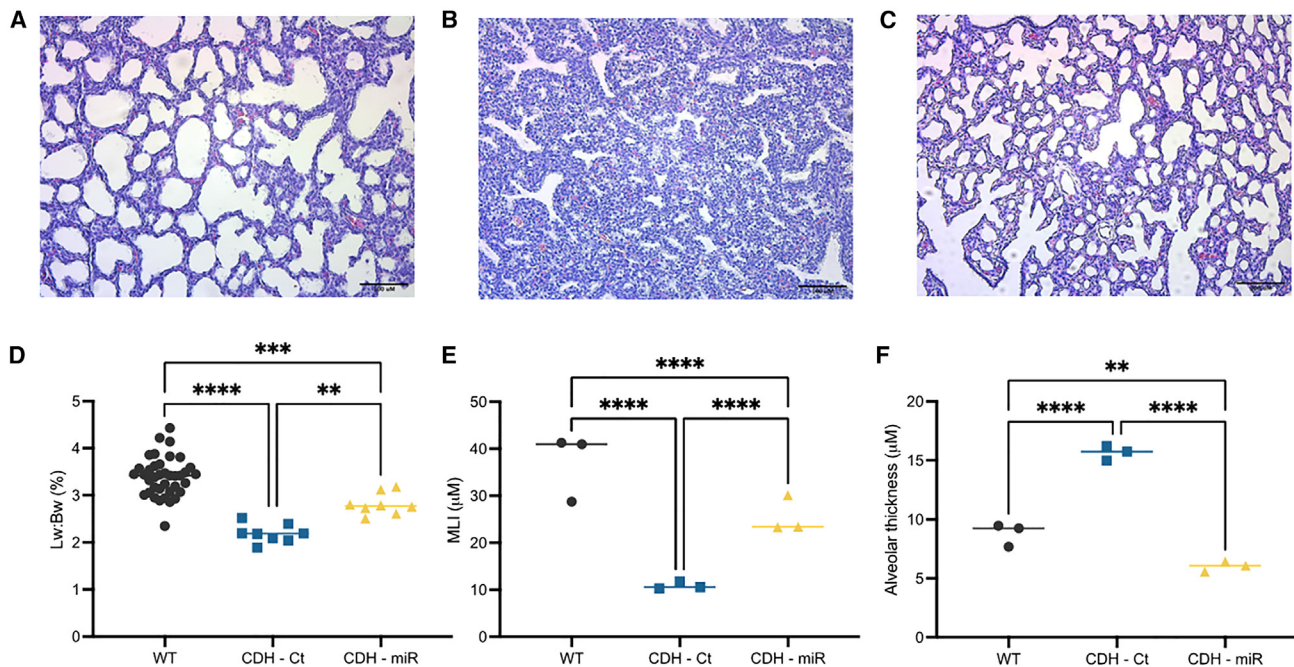
Figure 3. *In utero* delivery of miR200b PACE60 NPs improves pulmonary hypoplasia in the Nitrofen rat model of CDH

Representative hematoxylin and eosin images of (A) term WT lungs, (B) term CDH lungs treated with Control miRNA PACE60 NPs, and (C) term CDH lungs treated with miR200b PACE60 NPs. Scale bars, 100 µm. (D) Lung to body weight ratios of WT lungs, CDH lungs treated with control miRNA PACE60 NPs, and CDH lungs treated with miR200b PACE60 NPs. Each data point represents a single pup. One-way ANOVA, **p < 0.01, ***p < 0.001, ****p < 0.0001. (E) Mean linear intercept (MLI) of WT lungs, CDH lungs treated with control miRNA PACE60 NPs, and CDH lungs treated with miR200b PACE60 NPs. Each data point represents the lung of a single pup, averaging nine random fields per lung. One-way ANOVA, ****p < 0.0001. (F) Mean alveolar thickness of WT lungs, CDH lungs treated with control miRNA PACE60 NPs, and CDH lungs treated with miR200b PACE60 NPs. One-way ANOVA, **p < 0.01, ***p < 0.001, ****p < 0.0001. Each data point represents the lung of a single pup, averaging nine random fields per lung.

with miR200b had a 17.5% decrease in percent medial wall thicknesses compared with those treated with control NPs (43.5% vs. 52.7%, Figure 4D). The pulmonary arteries of pups treated with miR200b showed equivalent percent medial thicknesses to WT pups (Figure 4D).

In fetuses with PH without CDH, we do not see significant changes in lung size, lung morphology, or lung vasculature in the PH treated with miR200b NPs compared with those that are untreated (Figure S6).

DISCUSSION

In this study, we demonstrated that a single intravenous fetal dose of PACE60 NPs loaded with miR200b improves lung development in a rat model of CDH. Specifically, delivery of miR200b induced epigenetic changes related to the TGF-β pathway during the canalicular and saccular stages of pulmonary development. *In utero* treatment with miR200b led to larger lungs with more airspace and favorable pulmonary vascular remodeling at term in pups with CDH. This targeted, minimally invasive *in utero* strategy has the potential to avoid substantial antenatal morbidity and mortality in CDH.

We examined the relative expression of miR200b during the canalicular and saccular stages of rat lung development in both WT and CDH lungs and found that there is a marked deficiency in miR200b at E18, followed by an increase in relative expression leading to overexpression at E21. The relative expression of miR200b was equivalent at E19 and E20, suggesting that the early canalicular phase is an optimal time for delivery of miR200b. CDH is a devastating lung disease defined by impaired pulmonary vasculature and distal airway branching morphogenesis. miR200b plays a key role in this process, promoting distal airway development by maintaining an epithelial cell phenotype.[17,18,36,40] The role of miR200b in the pathogenesis of CDH has been less clearly delineated. Here, we defined a key role for miR200b in the pathogenesis of CDH. Our findings are consistent with previous findings, which examined miR200b expression in nitrofen-exposed lungs with varying degrees of hypoplasia.[18]

We demonstrated that, in the nitrofen rat model, the TGF-β pathway is upregulated in the lungs of pups with CDH relative to WT pups during the canalicular stage of lung development. During the transition from the canalicular to saccular stages, the TGF-β pathway is upregulated as branching morphogenesis slows down. However, in pups with CDH, the expression of the TGF-β pathway does not change significantly, further indicating that the dynamics of the TGF-β pathway is dysfunctional in the lungs of pups with CDH. The TGF-β pathway is one of many signal transduction pathways regulating
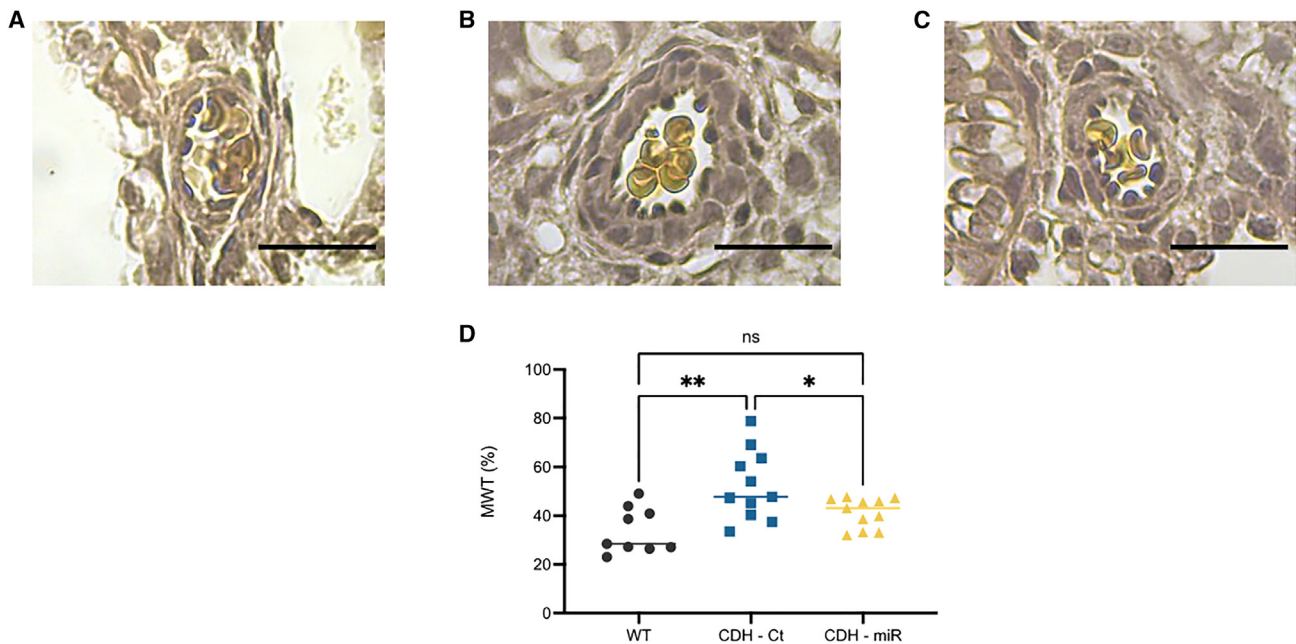
Figure 4. *In utero* delivery of miR200b PACE60 NPs results in pulmonary vascular remodeling in the Nitrofen rat model of CDH

Representative images of elastin van Gieson-stained pulmonary arteries from (A) term WT lungs, (B) term CDH lungs treated with control miRNA PACE60 NPs, and (C) term CDH lungs treated with miR200b PACE60 NPs. Scale bars, 20 μm. (D) Percent medial wall thickness of WT lungs, CDH lungs treated with control miRNA PACE60 NPs, and CDH lungs treated with miR200b PACE60 NPs. Each data point represents an individual arteriole. One-way ANOVA, **p < 0.01, ****p < 0.0001.

branching morphogenesis in the developing lung. TGF-β signaling is particularly important at the epithelial-mesenchymal interfaces during fetal development and plays a key role in branching morphogenesis.[16]

In this study, we demonstrated that *in utero* treatment with NPs loaded with miR200b can induce epigenetic changes in the fetal lung. Although treatments designed to modify tumor epigenetics have long been investigated for cancer, this has not been a focus of fetal interventions.[41] Treatment strategies that induce fetal epigenetic changes are particularly promising for CDH where—unlike other congenital pulmonary diseases such as cystic fibrosis—a monogenic cause has not been identified.[42] This suggests that environmental, epigenetic factors play a substantial role in the pathophysiology of CDH.

Fetal therapy for CDH, before a baby takes a first breath, is the optimal time to improve lung development as the lung is capable of structural change during fetal life and the gas exchange is managed by the placenta. We envision that NP-based fetal epigenetic therapy could be delivered through a small needle via ultrasound-guided cannulation of the umbilical vessels, which has been in clinical practice since the 1980s and carries a low risk of fetal loss (~1%).[43–45] In this study, miRNA is delivered at E17, which is equivalent gestational week 26 in the human fetus. Balloon deployment for FETO can occur as early as 27 weeks. However, therapies delivered via human umbilical vein cannulation can be delivered even earlier, at 16–18 weeks. Although FETO has been demonstrated to have a survival benefit for those with severe disease, it is an invasive procedure, and is associated with substantial risk of complications such as preterm premature rupture of the membranes and preterm delivery. Another major limitation of FETO is that, while it induces lung growth, it does not improve pulmonary vascular remodeling and pulmonary hypertension.[46] In this study, we demonstrated that *in utero* treatment with miR200b PACE60 NPs leads to favorable pulmonary vascular remodeling in addition to improving PH.

It has been previously reported that administration of a stabilized miR200b mimic into the maternal circulation at the time of teratogen exposure (E9.5) decreased the incidence of CDH and increased the mean linear intercept of non CDH pups. This study builds significantly on this existing literature. Gestational day E9.5 in the rat is equivalent to week 4 in human gestation, a time when most women do not even know they are pregnant and the diaphragm has not begun developing, making this a poor window for therapeutic intervention. Here, we are able to successfully deliver a therapeutic intervention at E17, which is equivalent to week 26 in human gestation where therapeutic intervention is possible. In addition, we deliver miR200b in a polymeric NP vector directly to the fetal circulation. This has several advantages including minimizing maternal miRNA exposure. We also demonstrated successful delivery of miRNA to the target tissues, which has not been the case previously. If translated to humans or large animals, this therapy can be administered directly to the fetus even earlier in gestation. We also demonstrate changes in gene expression, lung mass, pulmonary airspace and vascular remodeling, which is novel.

Table 1. Characterization data for PACE60 NP formulations

Formulation	Diameter (nm)	Polydispersity index	Zeta potential (mV)
PACE60 control miRNA	301 ± 3	0.170	30.2 ± 0.1
PACE60 miR200b	323 ± 2	0.190	31.2 ± 0.2

Although the PACE NPs used for this study have been optimized for delivery to fetal lung, there is still the potential for off-target effects.[33] Our previous studies demonstrated that, after *in utero* intravenous injection, the highest accumulation of polymeric NPs was in the fetal liver, with no detectable accumulation in the maternal tissues.[34,47] This study is significantly limited by the rodent model and further study involving large animal models is warranted. As this therapy is translated to larger animal models, direct intratracheal administration could be considered to minimize off-target delivery; intratracheal PACE vehicle delivery is well tolerated in adult animals.[48] This study demonstrates that a targeted, transient change in gene expression during lung development can lead to significant changes in pulmonary structure; however, the durability of these changes and long-term adverse effects still need to be determined. Analysis of pups at longer time points is warranted although not feasible in the nitrofen rat model of CDH, as pups typically expire within hours of birth.

We have demonstrated that miR200b delivery induces epigenetic changes related to the TGF-β pathway, although these are of unclear significance, indicating that other signal transduction pathways are impacted; further study is warranted before translation to larger animal models.[15] Success in such investigations could provide a strong foundation for clinical translation of this novel therapeutic modality.

MATERIALS AND METHODS

Polymer synthesis and NP formulation

PACE polymers were synthesized as described previously.[39] In brief, monomers (15-pentadecanolide, N-methyl diethanolamine, and diethyl sebacate) were dissolved in diphenyl ether with an enzyme lipase catalyst (Novozym 435). PDL (60 mol%) was used for the PACE polymer generated for this study. The synthesis reaction proceeded in two phases: an oligomerization phase for 18–20 h under argon at 1 atm, and then a polymerization phase for 48–72 h under vacuum. PACE polymers were characterized by NMR and GPC. PACE60 NPs were formulated as described previously by double emulsion solvent evaporation using miR200b mimic (Invitrogen *mir*Vana miRNA Mimic, hsa-miR-200b-3p, 5′- UAAUACUGCCUGGUAAUGAU GAC-3′, cat. no. 4464066, Ambion, Austin, TX) or a negative control miR (Invitrogen *mir*Vana miRNA Mimic, Negative Control 1, cat. no. 4464059, Ambion).[39,49] Characteristics of PACE60 NPs are displayed in Table 1.

Rat model and injection

All animal use was in accordance with the guidelines of the Animal Care and Use Committee of Yale University (IUCAC no. 2020–

11632). CDH was modeled in rats as described previously.[50] Time-dated pregnant Sprague-Dawley rats from Charles River Laboratories (Wilmington, MA) were gavage fed 100 mg of Nitrofen (cat. no. 33374, Sigma-Aldrich, St. Louis, MO) dissolved in olive oil (Whole Foods, Austin, TX) on embryonic day E9. Time-dated pregnant rats at 17 days post conception were anesthetized with inhaled isoflurane (2% vol/vol for induction and maintenance). E17 was selected for injection as it is the earliest time point when, in our experience, cannulation of the vitelline vein is technically feasible in the fetal rat. Analgesia was provided with subcutaneous injection of 0.3 mL buprenorphine HCl (0.015 mg/mL) and 0.3 mL meloxicam (0.1 mg/mL). The gravid uterus was exposed through a midline laparotomy incision. miR-loaded PACE60 NPs were resuspended by vortex and water bath sonication and delivered a dose of 30 mg/kg in 1× DPBS. NP suspension was drawn up into a glass micropipette (tip diameter ∼60 μm) and 15 μL of NP suspension was injected intravascularly via vitelline vein of each fetus using a pneumatic microinjector (Narishige, Japan). Rats were sacrificed at varying time points post injection and fetuses were delivered by cesarean section. In the nitrofen model, 50%–80% of pups exposed to nitrofen develop a left or right CDH and all pups display some degree of PH. For this analysis only pups with left-sided CDH with abdominal contents herniating into the thoracic cavity were selected. The incidence of CDH among treated groups is presented in Table S2. Data for pups exposed to nitrofen and did not develop a diaphragmatic hernia can be found in Figures S4–S6.

qRT-PCR

Total miRNA from fetal rat lung was extracted using the mirVana miRNA Isolation Kit (cat. no. AM1560, Ambion) according to the manufacturer's instructions. qRT-PCR was performed for miRNA 200b and its mRNA downstream targets.

For the miRNA assay, 1–10 ng total RNA were reverse transcribed using the TaqMan miRNA Assay for rno-miR200b-3p (rno481286_mir, cat. no. 4427975, Applied Biosystems, Foster City, CA) TaqMan Advanced miRNA cDNA Synthesis Kit (cat. no. A28007, Applied Biosystems) following the manufacturer's protocol as described. qRT-PCR was performed using the TaqMan Fast Advanced Master Mix (cat. no. 4444556, Applied Biosystems). U6 snRNA (cat. no. 4444556, Applied Biosystems) was used for normalization.

qRT-PCR of mRNA was performed using the Applied Biosystems predesigned TaqMan Gene Expression Assays (cat. no. 4331182, Applied Biosystems), and Superscript IV VILO Master Mix (cat. no. 11766050, Invitrogen, Carlsbad, CA) per the manufacturer's instructions for rat glyceraldehyde-3-phosphate dehydrogenase (Gapdh; Rn01462662_g1), transforming growth factor beta 1 (Tgfb1; Rn00665219_g1), transforming growth factor beta 2 (Tgfb1; Rn00579674_m1), zinc finger E-box binding homeobox 1 (Zeb1; Rn01538408_m1), zinc finger E-box binding homeobox 2 (Zeb2; Rn01449758_m1), SMAD family member 2 (Smad2; Rn015 27104_g1), and SMAD family member 3 (Smad3; Rn01422011_m1).

Lung morphometry

Fetal rats were delivered by cesarean section on E21 and lung:body weight ratio was measured. For morphometric analysis, fetal lungs were fixed by intratracheal instillation of 4% paraformaldehyde under a constant pressure of 20 cm H_2O for 5 min. Visual confirmation of inflation was obtained for all specimens analyzed. After ligation of the trachea, the entire left lung was immersed in fixative and embedded in paraffin. Sections from medial, mid, and lateral lung zones were mounted onto slides and stained with hematoxylin and eosin or elastin van Gieson's (EvG) stain.[51] The slides were imaged on a Zeiss Axio Scope light microscope (Carl Zeiss Microscopy, Germany).

Airspace enlargement was measured by assessing mean linear intercept (Lm) by a blinded reviewer (Figure S7). Three random fields verified to not contain major airways or vasculature were selected from mid, medial, and lateral lung sections resulting in a total of nine random fields per lung. Lungs were evaluated by microscopic projection and the alveolar size was estimated from the Lm of the airspace as described previously.[52–55] Care was taken to exclude the volume occupied by the septa and limit the measurement to airspaces. Alveolar thickness was measured as the mean septal wall thickness of 10 terminal alveoli per field (Figure S7).

EvG-stained sections were used for pulmonary arteriole (PA) remodeling assessment. The PAs were distinguished from pulmonary veins based on their position and structure. In each sample, only small PAs (external diameter [ED]: 20–100 μm) were used. ED was measured across the shortest luminal profile between the external elastic laminae by a blinded reviewer. Diameter across the longest luminal profile also was measured, and only arteries in which the longest diameter did not exceed ED by more than 50% were used. Medial thickness was measured on the same profile as ED. To assess PA remodeling, the percentage of the medial wall thickness was calculated according to the following formula: $(2 \times \text{medial wall thickness}/\text{external diameter}) \times 100\%$, as described previously.[56–58]

Statistical analysis

Data are presented as means ± SD unless otherwise noted and compared using Student's t test, or one- or two-way ANOVA followed by Tukey's post-hoc test for multiple comparisons when appropriate. Bonferroni correction was used to correct for multiple comparisons. Statistical analyses were carried out using GraphPad Prism v.9. A p value of less than 0.05 was considered statistically significant.

DATA AVAILABILITY

The data that support the findings of this study are available from the corresponding author.

SUPPLEMENTAL INFORMATION

Supplemental information can be found online at https://doi.org/10.1016/j.omtn.2023.04.018.

AUTHOR CONTRIBUTIONS

Conceptualization, S.J.U., A.S.R., W.M.S., A.S.P.-D., and D.H.S.; data curation, S.J.U. and T.J.B.-P.; formal analysis, S.J.U., M.E.G., and M.S.; investigation, S.J.U., N.K.Y., T.J.B.-P., N.L.M., M.F.-W., S.L.A., and A.S.P.-D.; methodology, S.J.U., A.S.R., M.S., W.M.S., A.S.P.-D., and D.H.S.; project administration, S.J.U. and N.K.Y.; visualization, S.J.U. and N.K.Y.; writing – original draft, S.J.U.; writing – review & editing, S.J.U., M.S., W.M.S., A.S.P.-D., and D.H.S.; funding acquisition, S.L.A., M.S., W.M.S., A.S.P.-D., and D.H.S.; supervision, A.S.R., M.S., W.M.S., A.S.P.-D., and D.H.S.; resources, W.M.S. and D.H.S.; project administration, D.H.S.

DECLARATION OF INTERESTS

S.J.U., W.M.S., A.S.R., D.H.S., and A.S.P.-D. have filed an invention disclosure for the technology used in this manuscript with the Yale Office of Cooperative Research. W.M.S., A.S.R., D.H.S., and A.S.P.-D. are listed as inventors on the following patent: https://patents.justia.com/patent/20200113821.

REFERENCES

1. Longoni, M., High, F.A., Russell, M.K., Kashani, A., Tracy, A.A., Coletti, C.M., Hila, R., Shamia, A., Wells, J., Ackerman, K.G., et al. (2014). Molecular pathogenesis of congenital diaphragmatic hernia revealed by exome sequencing, developmental data, and bioinformatics. Proc. Natl. Acad. Sci. USA *111*, 12450–12455. https://doi.org/10.1073/pnas.1412509111.

2. Veenma, D.C.M., de Klein, A., and Tibboel, D. (2012). Developmental and genetic aspects of congenital diaphragmatic hernia. Pediatr. Pulmonol. *47*, 534–545. https://doi.org/10.1002/ppul.22553.

3. Langham, M.R., Kays, D.W., Ledbetter, D.J., Frentzen, B., Sanford, L.L., and Richards, D.S. (1996). Congenital diaphragmatic hernia: epidemiology and outcome. Clin. Perinatol. *23*, 671–688. https://doi.org/10.1016/S0095-5108(18)30201-X.

4. Wynn, J., Krishnan, U., Aspelund, G., Zhang, Y., Duong, J., Stolar, C.J.H., Hahn, E., Pietsch, J., Chung, D., Moore, D., et al. (2013). Outcomes of congenital diaphragmatic hernia in the modern era of management. J. Pediatr. *163*, 114–119.e1. https://doi.org/10.1016/j.jpeds.2012.12.036.

5. Coughlin, M.A., Werner, N.L., Gajarski, R., Gadepalli, S., Hirschl, R., Barks, J., Treadwell, M.C., Ladino-Torres, M., Kreutzman, J., and Mychaliska, G.B. (2016). Prenatally diagnosed severe CDH: mortality and morbidity remain high. J. Pediatr. Surg. *51*, 1091–1095. https://doi.org/10.1016/j.jpedsurg.2015.10.082.

6. McGivern, M.R., Best, K.E., Rankin, J., Wellesley, D., Greenlees, R., Addor, M.C., Arriola, L., de Walle, H., Barisic, I., Beres, J., et al. (2015). Epidemiology of congenital diaphragmatic hernia in Europe: a register-based study. Arch. Dis. Child. Fetal Neonatal Ed. *100*, F137–F144. https://doi.org/10.1136/archdischild-2014-306174.

7. Ameis, D., Khoshgoo, N., and Keijzer, R. (2017). Abnormal lung development in congenital diaphragmatic hernia. Semin. Pediatr. Surg. 26, 123–128. https://doi.org/10.1053/j.sempedsurg.2017.04.011.

8. Donahoe, P.K., Longoni, M., and High, F.A. (2016). Polygenic causes of congenital diaphragmatic hernia produce common lung pathologies. Am. J. Pathol. 186, 2532–2543. https://doi.org/10.1016/j.ajpath.2016.07.006.

9. George, D.K., Cooney, T.P., Chiu, B.K., and Thurlbeck, W.M. (1987). Hypoplasia and immaturity of the terminal lung unit (acinus) in congenital diaphragmatic hernia. Am. Rev. Respir. Dis. 136, 947–950. https://doi.org/10.1164/ajrccm/136.4.947.

10. Kool, H., Mous, D., Tibboel, D., de Klein, A., and Rottier, R.J. (2014). Pulmonary vascular development goes awry in congenital lung abnormalities. Birth Defects Res. C Embryo Today. 102, 343–358. https://doi.org/10.1002/bdrc.21085.

11. Deprest, J.A., Nicolaides, K.H., Benachi, A., Gratacos, E., Ryan, G., Persico, N., Sago, H., Johnson, A., Wielgoś, M., Berg, C., et al. (2021). Randomized trial of fetal Surgery for severe left diaphragmatic hernia. N. Engl. J. Med. 385, 107–118. https://doi.org/10.1056/NEJMoa2027030.

12. Deprest, J.A., Benachi, A., Gratacos, E., Nicolaides, K.H., Berg, C., Persico, N., Belfort, M., Gardener, G.J., Ville, Y., Johnson, A., et al. (2021). Randomized trial of fetal Surgery for moderate left diaphragmatic hernia. N. Engl. J. Med. 385, 119–129. https://doi.org/10.1056/NEJMoa2026983.

13. Pereira-Terra, P., Deprest, J.A., Kholdebarin, R., Khoshgoo, N., DeKoninck, P., Munck, A.A., Wang, J., Zhu, F., Rottier, R.J., Iwasiow, B.M., et al. (2015). Unique tracheal fluid MicroRNA signature predicts response to FETO in patients with congenital diaphragmatic hernia. Ann. Surg. 262, 1130–1140. https://doi.org/10.1097/sla.0000000000001054.

14. Burk, U., Schubert, J., Wellner, U., Schmalhofer, O., Vincan, E., Spaderna, S., and Brabletz, T. (2008). A reciprocal repression between ZEB1 and members of the miR-200 family promotes EMT and invasion in cancer cells. EMBO Rep. 9, 582–589. https://doi.org/10.1038/embor.2008.74.

15. Gregory, P.A., Bracken, C.P., Smith, E., Bert, A.G., Wright, J.A., Roslan, S., Morris, M., Wyatt, L., Farshid, G., Lim, Y.Y., et al. (2011). An autocrine TGF-beta/ZEB/miR-200 signaling network regulates establishment and maintenance of epithelial-mesenchymal transition. Mol. Biol. Cell 22, 1686–1698. https://doi.org/10.1091/mbc.E11-02-0103.

16. Lü, J., Qian, J., Izvolsky, K.I., and Cardoso, W.V. (2004). Global analysis of genes differentially expressed in branching and non-branching regions of the mouse embryonic lung. Dev. Biol. 273, 418–435. https://doi.org/10.1016/j.ydbio.2004.05.035.

17. Khoshgoo, N., Visser, R., Falk, L., Day, C.A., Ameis, D., Iwasiow, B.M., Zhu, F., Öztürk, A., Basu, S., Pind, M., et al. (2017). MicroRNA-200b regulates distal airway development by maintaining epithelial integrity. Sci. Rep. 7, 6382. https://doi.org/10.1038/s41598-017-05412-y.

18. Khoshgoo, N., Kholdebarin, R., Pereira-Terra, P., Mahood, T.H., Falk, L., Day, C.A., Iwasiow, B.M., Zhu, F., Mulhall, D., Fraser, C., et al. (2019). Prenatal microRNA miR-200b therapy improves nitrofen-induced pulmonary hypoplasia associated with congenital diaphragmatic hernia. Ann. Surg. 269, 979–987. https://doi.org/10.1097/sla.0000000000002595.

19. Rupaimoole, R., and Slack, F.J. (2017). MicroRNA therapeutics: towards a new era for the management of cancer and other diseases. Nat. Rev. Drug Discov. 16, 203–222. https://doi.org/10.1038/nrd.2016.246.

20. Rupaimoole, R., Han, H.D., Lopez-Berestein, G., and Sood, A.K. (2011). MicroRNA therapeutics: principles, expectations, and challenges. Chin. J. Cancer 30, 368–370. https://doi.org/10.5732/cjc.011.10186.

21. Li, Z., and Rana, T.M. (2014). Therapeutic targeting of microRNAs: current status and future challenges. Nat. Rev. Drug Discov. 13, 622–638. https://doi.org/10.1038/nrd4359.

22. van Rooij, E., and Kauppinen, S. (2014). Development of microRNA therapeutics is coming of age. EMBO Mol. Med. 6, 851–864. https://doi.org/10.15252/emmm.201100899.

23. Blum, J.S., and Saltzman, W.M. (2008). High loading efficiency and tunable release of plasmid DNA encapsulated in submicron particles fabricated from PLGA conjugated with poly-L-lysine. J. Control. Release 129, 66–72. https://doi.org/10.1016/j.jconrel.2008.04.002.

24. Trang, P., Wiggins, J.F., Daige, C.L., Cho, C., Omotola, M., Brown, D., Weidhaas, J.B., Bader, A.G., and Slack, F.J. (2011). Systemic delivery of tumor suppressor microRNA mimics using a neutral lipid emulsion inhibits lung tumors in mice. Mol. Ther. 19, 1116–1122. https://doi.org/10.1038/mt.2011.48.

25. Ozpolat, B., Sood, A.K., and Lopez-Berestein, G. (2010). Nanomedicine based approaches for the delivery of siRNA in cancer. J. Intern. Med. 267, 44–53. https://doi.org/10.1111/j.1365-2796.2009.02191.x.

26. Joshi, H.P., Subramanian, I.V., Schnettler, E.K., Ghosh, G., Rupaimoole, R., Evans, C., Saluja, M., Jing, Y., Cristina, I., Roy, S., et al. (2014). Dynamin 2 along with microRNA-199a reciprocally regulate hypoxia-inducible factors and ovarian cancer metastasis. Proc. Natl. Acad. Sci. USA 111, 5331–5336. https://doi.org/10.1073/pnas.1317242111.

27. Dahlman, J.E., Barnes, C., Khan, O., Thiriot, A., Jhunjunwala, S., Shaw, T.E., Xing, Y., Sager, H.B., Sahay, G., Speciner, L., et al. (2014). In vivo endothelial siRNA delivery using polymeric nanoparticles with low molecular weight. Nat. Nanotechnol. 9, 648–655. https://doi.org/10.1038/nnano.2014.84.

28. Woodrow, K.A., Cu, Y., Booth, C.J., Saucier-Sawyer, J.K., Wood, M.J., and Saltzman, W.M. (2009). Intravaginal gene silencing using biodegradable polymer nanoparticles densely loaded with small-interfering RNA. Nat. Mater. 8, 526–533. https://doi.org/10.1038/nmat2444.

29. Piotrowski-Daspit, A.S., Kauffman, A.C., Bracaglia, L.G., and Saltzman, W.M. (2020). Polymeric vehicles for nucleic acid delivery. Adv. Drug Deliv. Rev. 156, 119–132. https://doi.org/10.1016/j.addr.2020.06.014.

30. Lv, H., Zhang, S., Wang, B., Cui, S., and Yan, J. (2006). Toxicity of cationic lipids and cationic polymers in gene delivery. J. Control. Release 114, 100–109. https://doi.org/10.1016/j.jconrel.2006.04.014.

31. Makadia, H.K., and Siegel, S.J. (2011). Poly lactic-co-glycolic acid (PLGA) as biodegradable controlled drug delivery carrier. Polymers 3, 1377–1397. https://doi.org/10.3390/polym3031377.

32. Zhou, J., Liu, J., Cheng, C.J., Patel, T.R., Weller, C.E., Piepmeier, J.M., Jiang, Z., and Saltzman, W.M. (2011). Biodegradable poly(amine-co-ester) terpolymers for targeted gene delivery. Nat. Mater. 11, 82–90. https://doi.org/10.1038/nmat3187.

33. Ullrich, S.J., Freedman-Weiss, M., Ahle, S., Mandl, H.K., Piotrowski-Daspit, A.S., Roberts, K., Yung, N., Maassel, N., Bauer-Pisani, T., Ricciardi, A.S., et al. (2021). Nanoparticles for delivery of agents to fetal lungs. Acta Biomater. 123, 346–353. https://doi.org/10.1016/j.actbio.2021.01.024.

34. Ricciardi, A.S., Bahal, R., Farrelly, J.S., Quijano, E., Bianchi, A.H., Luks, V.L., Putman, R., López-Giráldez, F., Coşkun, S., Song, E., et al. (2018). In Utero nanoparticle delivery for site-specific genome editing. Nat. Commun. 9, 2481. https://doi.org/10.1038/s41467-018-04894-2.

35. Schittny, J.C. (2017). Development of the lung. Cell Tissue Res. 367, 427–444. https://doi.org/10.1007/s00441-016-2545-0.

36. Alejandre-Alcázar, M.A., Michiels-Corsten, M., Vicencio, A.G., Reiss, I., Ryu, J., de Krijger, R.R., Haddad, G.G., Tibboel, D., Seeger, W., Eickelberg, O., et al. (2008). TGF-beta signaling is dynamically regulated during the alveolarization of rodent and human lungs. Dev. Dynam. 237, 259–269. an official publication of the American Association of Anatomists. https://doi.org/10.1002/dvdy.21403.

37. Chen, H., Sun, J., Buckley, S., Chen, C., Warburton, D., Wang, X.F., and Shi, W. (2005). Abnormal mouse lung alveolarization caused by Smad3 deficiency is a developmental antecedent of centrilobular emphysema. Am. J. Physiol. Lung Cell Mol. Physiol. 288, L683–L691. https://doi.org/10.1152/ajplung.00298.2004.

38. Mous, D.S., Buscop-van Kempen, M.J., Wijnen, R.M.H., Tibboel, D., Morty, R.E., and Rottier, R.J. (2021). Opposing effects of TGFβ and BMP in the pulmonary vasculature in congenital diaphragmatic hernia. Front. Med. 8, 642577. https://doi.org/10.3389/fmed.2021.642577.

39. Kauffman, A.C., Piotrowski-Daspit, A.S., Nakazawa, K.H., Jiang, Y., Datye, A., and Saltzman, W.M. (2018). Tunability of biodegradable poly(amine- co-ester) polymers for customized nucleic acid delivery and other biomedical applications. Biomacromolecules 19, 3861–3873. https://doi.org/10.1021/acs.biomac.8b00997.

40. Chinoy, M.R. (2003). Lung growth and development. Front. Biosci. 8, d392–d415. https://doi.org/10.2741/974.

41. Bates, S.E. (2020). Epigenetic therapies for cancer. N. Engl. J. Med. 383, 650–663. https://doi.org/10.1056/NEJMra1805035.

42. Wagner, R., Montalva, L., Zani, A., and Keijzer, R. (2020). Basic and translational science advances in congenital diaphragmatic hernia. Semin. Perinatol. 44, 151170. https://doi.org/10.1053/j.semperi.2019.07.009.

43. Van Kamp, I.L., Klumper, F.J.C.M., Oepkes, D., Meerman, R.H., Scherjon, S.A., Vandenbussche, F.P., and Kanhai, H.H. (2005). Complications of intrauterine intravascular transfusion for fetal anemia due to maternal red-cell alloimmunization. Am. J. Obstet. Gynecol. 192, 171–177. https://doi.org/10.1016/j.ajog.2004.06.063.

44. Bang, J., Bock, J.E., and Trolle, D. (1982). Ultrasound-guided fetal intravenous transfusion for severe rhesus haemolytic disease. Br. Med. J. 284, 373–374.

45. Pasman, S.A., Claes, L., Lewi, L., Van Schoubroeck, D., Debeer, A., Emonds, M., Geuten, E., De Catte, L., and Devlieger, R. (2015). Intrauterine transfusion for fetal anemia due to red blood cell alloimmunization: 14 years experience in Leuven. Facts Views Vis. Obgyn 7, 129–136.

46. Perrone, E.E., and Deprest, J.A. (2021). Fetal endoscopic tracheal occlusion for congenital diaphragmatic hernia: a narrative review of the history, current practice, and future directions. Transl. Pediatr. 10, 1448–1460. https://doi.org/10.21037/tp-20-130 (2021.

47. Luks, V.L., Mandl, H., DiRito, J., Barone, C., Freedman-Weiss, M.R., Ricciardi, A.S., Tietjen, G.G., Egan, M.E., Saltzman, W.M., and Stitelman, D.H. (2022). Surface conjugation of antibodies improves nanoparticle uptake in bronchial epithelial cells. PLoS One 17, e0266218. https://doi.org/10.1371/journal.pone.0266218.

48. Grun, M.K., Suberi, A., Shin, K., Lee, T., Gomerdinger, V., Moscato, Z.M., Piotrowski-Daspit, A.S., and Saltzman, W.M. (2021). PEGylation of poly(amine-co-ester) polyplexes for tunable gene delivery. Biomaterials 272, 120780. https://doi.org/10.1016/j.biomaterials.2021.120780.

49. Cui, J., Piotrowski-Daspit, A.S., Zhang, J., Shao, M., Bracaglia, L.G., Utsumi, T., Seo, Y.E., DiRito, J., Song, E., Wu, C., et al. (2019). Poly(amine-co-ester) nanoparticles for effective Nogo-B knockdown in the liver. J. Control. Release 304, 259–267. https://doi.org/10.1016/j.jconrel.2019.04.044.

50. Kluth, D., Kangah, R., Reich, P., Tenbrinck, R., Tibboel, D., and Lambrecht, W. (1990). Nitrofen-induced diaphragmatic hernias in rats: an animal model. J. Pediatr. Surg. 25, 850–854. https://doi.org/10.1016/0022-3468(90)90190-k.

51. Burgos, C.M., Pearson, E.G., Davey, M., Riley, J., Jia, H., Laje, P., Flake, A.W., and Peranteau, W.H. (2016). Improved pulmonary function in the nitrofen model of congenital diaphragmatic hernia following prenatal maternal dexamethasone and/or sildenafil. Pediatr. Res. 80, 577–585. https://doi.org/10.1038/pr.2016.127.

52. Knudsen, L., Weibel, E.R., Gundersen, H.J.G., Weinstein, F.V., and Ochs, M. (2010). Assessment of air space size characteristics by intercept (chord) measurement: an accurate and efficient stereological approach. J. Appl. Physiol. 108, 412–421. https://doi.org/10.1152/japplphysiol.01100.2009.

53. Thurlbeck, W.M. (1967). Internal surface area and other measurements in emphysema. Thorax 22, 483–496. https://doi.org/10.1136/thx.22.6.483.

54. Kim, S.J., Shan, P., Hwangbo, C., Zhang, Y., Min, J.N., Zhang, X., Ardito, T., Li, A., Peng, T., Sauler, M., and Lee, P.J. (2019). Endothelial toll-like receptor 4 maintains lung integrity via epigenetic suppression of p16(INK4a). Aging Cell 18, e12914. https://doi.org/10.1111/acel.12914.

55. Hsia, C.C.W., Hyde, D.M., Ochs, M., and Weibel, E.R.; ATS/ERS Joint Task Force on Quantitative Assessment of Lung Structure (2010). An official research policy statement of the American Thoracic Society/European Respiratory Society: standards for quantitative assessment of lung structure. Am. J. Respir. Crit. Care Med. 181, 394–418. https://doi.org/10.1164/rccm.200809-1522ST.

56. Kanai, M., Kitano, Y., von Allmen, D., Davies, P., Adzick, N.S., and Flake, A.W. (2001). Fetal tracheal occlusion in the rat model of nitrofen-induced congenital diaphragmatic hernia: tracheal occlusion reverses the arterial structural abnormality. J. Pediatr. Surg. 36, 839–845. https://doi.org/10.1053/jpsu.2001.23950.

57. Umeda, S., Miyagawa, S., Fukushima, S., Oda, N., Saito, A., Sakai, Y., Sawa, Y., and Okuyama, H. (2016). Enhanced pulmonary vascular and alveolar development via prenatal administration of a slow-release synthetic prostacyclin agonist in rat fetal lung hypoplasia. PLoS One 11, e0161334. https://doi.org/10.1371/journal.pone.0161334.

58. Xu, X.F., Gu, W.Z., Wu, X.L., Li, R.Y., and Du, L.Z. (2011). Fetal pulmonary vascular remodeling in a rat model induced by hypoxia and indomethacin. J. Matern. Fetal Neonatal Med. 24, 172–182. https://doi.org/10.3109/14767058.2010.482608.